

Cite this: *Chem. Sci.*, 2022, 13, 10891

All publication charges for this article have been paid for by the Royal Society of Chemistry

Received 3rd May 2022

Accepted 9th August 2022

DOI: 10.1039/d2sc02485c

rsc.li/chemical-science

Generation of boryl-nitroxide radicals from a boraalkene *via* the nitroso ene reaction†

Chaohuang Chen,^a Constantin G. Daniliuc,^a Sina Klabunde,^b Michael Ryan Hansen,^b Gerald Kehr^a and Gerhard Erker^{a*}

Examples of isolated boron substituted nitroxide radicals are rare. The reaction of the reactive cyclic boraalkene **3** with nitrosobenzene yields a mixture of the [2 + 2] cycloaddition product **4a**, the *B*-nitroxide radicals **5a** and **6a** and the azoxybenzene co-product **7a** *via* a bora nitroso ene reaction pathway, the boron analogue of the nitroso ene reaction. The products were separated by flash chromatography, and the *B*-nitroxide radicals were characterized by X-ray diffraction and EPR spectroscopy. Radical **5a** was shown to be a hydrogen atom abstractor. Both the *B*-nitroxide radicals are more easily oxidized compared to e.g. TEMPO, as shown by cyclic voltammetry.

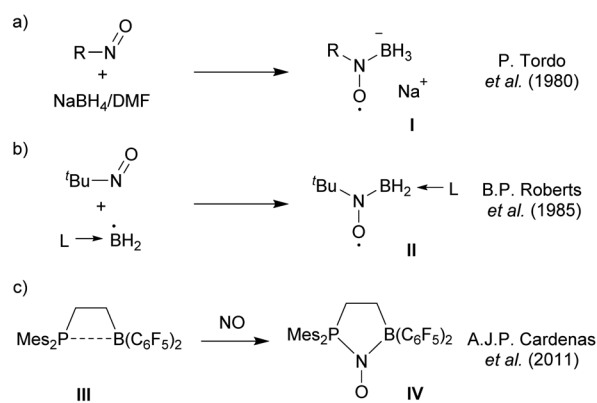
Introduction

Nitroxide radicals are an important class of compounds. The TEMPO aminoxyl radical and its derivatives have found extensive use in organic and polymerization chemistry and beyond.¹ The defined redox chemistry of the nitroxide radicals has been used in stoichiometric and catalytic oxidation processes,² and nitroxides have been employed as ligands in transition metal coordination chemistry.³ While numerous substituted and functionalized aminoxyl radicals have become known, examples of boron containing nitroxide radicals are less frequently encountered.^{4–9}

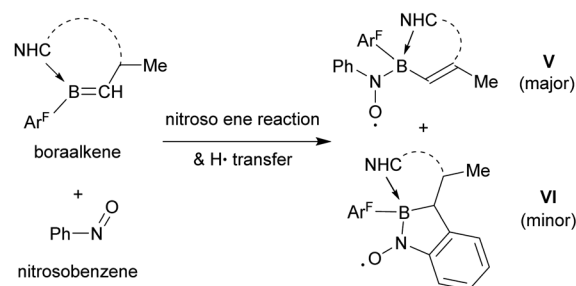
Tordo *et al.* reported the generation of the nitroxide radical anion **I** by treatment of 2-methyl-2-nitrosopropane with NaBH₄/DMF (Scheme 1a).⁵ The *in situ* generated BH₃[–] radical anion was detected using spin traps.⁶ B. P. Roberts *et al.*⁷ used a number of nitroso alkanes and nitroso arenes as spin traps to successfully detect a variety of ligated ·BH₂ radicals⁸ as verified by EPR spectroscopy (Scheme 1b). Our group had used the special features of frustrated Lewis pair (FLP) chemistry to prepare persistent *P/B*-nitroxide radicals, that were isolated and characterized by spectroscopy and by X-ray crystal structure analysis. The formation of compound **IV** *via* exposure of the intramolecular ethylene bridged *P/B* FLP **III** to nitric oxide under mild conditions is a typical example (Scheme 1c).⁹

We have now found that examples of boryl-nitroxide radicals can be made by treatment of a suitably substituted boraalkene with nitrosobenzene by a pathway that involves a variant of the nitroso ene reaction.¹⁰ The radicals of type **V** and **VI** were obtained as examples of this class of compounds. They were thoroughly characterized including EPR spectroscopy and X-ray diffraction (Scheme 1d).

previous works



d) this work



Scheme 1 Examples of boron containing nitroxide radicals.

^aOrganisch-Chemisches Institut, Westfälische Wilhelms-Universität Münster, Corrensstraße 40, 48149 Münster, Germany. E-mail: erker@uni-muenster.de

^bInstitut für Physikalische Chemie, Westfälische Wilhelms-Universität Münster, Corrensstraße 28/3040, 48149 Münster, Germany

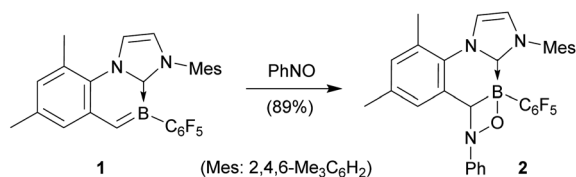
† Electronic supplementary information (ESI) available: Experimental procedures and details on the characterization of the new compounds. CCDC 2157861 (**2**), 2157862 (**4a**), 2182533 (**4c_{ax}**), 2157863 (**5a**), 2157864 (**6a**), 2157865 (**9**), and 2157866 (**13**). For ESI and crystallographic data in CIF or other electronic format see <https://doi.org/10.1039/d2sc02485c>

Results and discussion

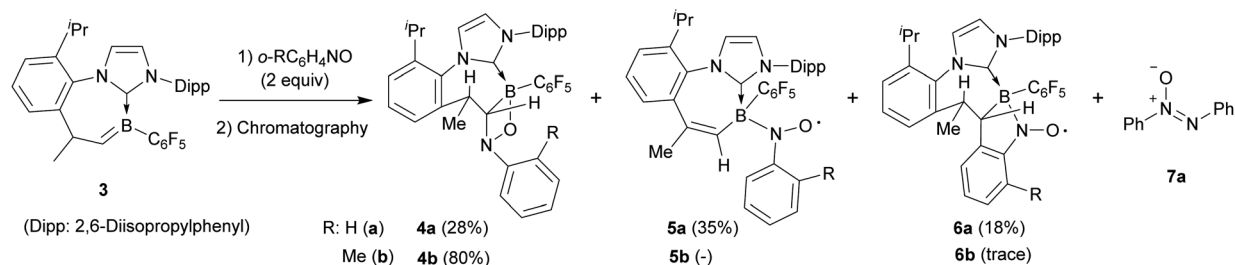
We had described that cyclic boraalkene **1** was readily prepared starting from the corresponding $[(\text{IMes})(\text{C}_6\text{F}_5)\text{BH}]^+$ borenium cation (with the $[\text{B}(\text{C}_6\text{F}_5)_4]^-$ anion)¹¹ by a sequence involving thermally induced intramolecular C–H activation at an *ortho*-methyl group of an NHC mesityl substituent (with H_2 formation) followed by deprotonation.¹² Compound **1** was now found to rapidly react with nitrosobenzene¹³ (C_6D_6 , r.t., 5 min) to yield the $[2 + 2]$ cycloaddition product **2** (see Scheme 2).

The X-ray crystal structure analysis of compound **2** showed bond lengths inside the newly formed four-membered heterocycle of 1.505(4) Å (B1–O1), 1.624(4) Å (B1–C17), 1.504(3) Å (N3–C17) and 1.475(3) Å (N3–O1). In solution (C_6D_6), this unit showed NMR features at δ –4.1 (^{11}B) and δ 69.1/4.57 ($^{13}\text{C}/^1\text{H}$), respectively (see the ESI† for further details and the depicted structure).

Boraalkene **3** was prepared from the corresponding borenium salt $[(\text{iPr})(\text{C}_6\text{F}_5)\text{BH}]^+[\text{B}(\text{C}_6\text{F}_5)_4]^-$ by a procedure analogous to the formation of **1**, as previously described.¹² Boraalkene **3** was reacted with 2 molar equiv. of nitrosobenzene. After a reaction time of 1 h (r.t. in C_6D_6), the components of the product mixture were separated by gradient elution flash chromatography. In this case, the $[2 + 2]$ cycloaddition product (**4a**, isolated as an off-white solid in 28% yield) was not the sole product in contrast to the above described nitrosobenzene reaction with boraalkene **1**. The major product isolated was the persistent nitroxide radical **5a** (35% yield), and it was accompanied by the isomeric nitroxide radical **6a** in a yield of 18%. Azoxybenzene **7a** was obtained as a necessary co-product of the nitroxide radical formation (see Scheme 3).¹⁴ In a second experiment, it was shown that compounds **4a–6a** could also be obtained by treating compound **3** with 1 equiv. of nitrosobenzene and subsequent exposure to air (see the ESI† for details).



Scheme 2 Reaction of cyclic boraalkene **1** with nitrosobenzene.



Scheme 3 Formation of two boryl-nitroxide radicals **5a** and **6a** from the reaction of the cyclic NHC-stabilized boraalkene **3** with nitrosobenzene. The yields given refer to the isolated material (see the ESI† for details).

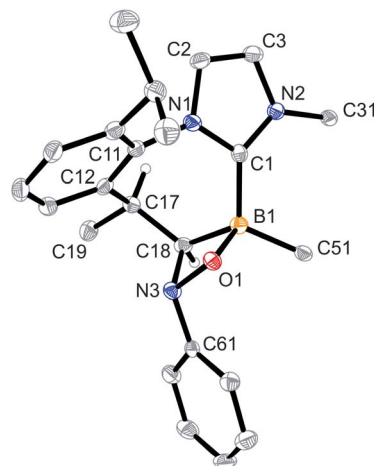


Fig. 1 A view of the molecular structure of the boraalkene/nitrosobenzene $[2 + 2]$ cycloaddition product **4a** [thermal ellipsoids are set at 50% probability; only the *ipso*- C_6F_5 /Dipp carbon atoms C51/C31 are shown for clarity, and H atoms are omitted (except for C17H and C18H)]. Selected bond lengths (Å) and angles ($^\circ$): B1–O1 1.512(2), B1–C1 1.619(3), B1–C18 1.636(3), C17–C18 1.547(2), O1–N3 1.481(2), N3–C18 1.503(2), C18–N3–O1 93.6(1), C19–C17–C18–N3 –86.2(2), C18–N3–O1–B1 –16.5(1), and $\Sigma\text{N}3^{\text{CCO}}$ 330.0.

The products **4a–6a** were obtained crystalline and characterized by X-ray crystal structure analysis. The structure of the PhNO adduct **4a** (see Fig. 1) shows the newly formed CNOB containing four-membered heterocyclic ring system annulated with the central seven-membered core that had been generated by the initial C–H activation process during the synthesis of the starting material **3**. The seven-membered heterocycle shows a boat-shaped conformation with the methyl substituent at its saturated $\text{C}(\text{sp}^3)$ tip oriented equatorially.

In solution (CD_2Cl_2 , 299 K), compound **4a** shows a ^{11}B NMR signal at δ –0.7. The NMR signals of the CH group inside the annulated four-membered heterocyclic ring system occur at 80.7 (^{13}C) and 3.44 (^1H), respectively.

Crystallization of the obtained brown solid from CH_2Cl_2 /pentane gave compound **5a** as dark-red crystals. The X-ray crystal structure analysis of the nitroxide radical **5a** (see Fig. 2) also shows a central 1,3-azaborepine derived core, but in this case, the boron atom represents the tip of the boat-shaped structure. Adjacent to it are a newly formed endo-cyclic carbon–carbon double bond and the N–C moiety of the annulated



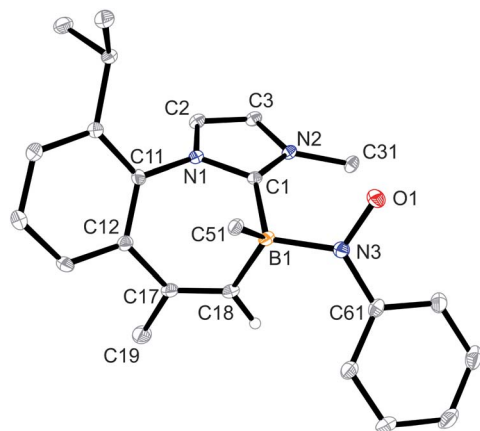


Fig. 2 Molecular structure of the BNO nitroxide radical **5a** [thermal ellipsoids are set at 30% probability; only the *ipso*-C₆F₅/Dipp carbon atoms C51/C31 are shown for clarity, and H atoms are omitted (except for C18H)]. Selected bond lengths (Å) and angles (°): B1–C1 1.631(2), B1–C18 1.615(2), B1–N3 1.558(2), C17–C18 1.339(2), N3–O1 1.304(2), B1–N3–O1 115.4(1), C1–B1–N3–O1 54.0(2), and $\Sigma N3^{BCO}$ 359.9.

imidazolyliene unit. The Dipp derived annulated isopropylphenylene unit is oriented at the distal position to the boron tip. Boron atom B1 bears the C₆F₅ substituent and the newly formed –N(–O)Ph nitroxide radical building block. The latter is found in an equatorial orientation at the central seven-membered ring. Compound **5a** represents a rare example of a boron substituted persistent nitroxide radical. Its B–N–O subunit shows bond lengths of 1.558(2) Å (B1–N3) and 1.304(2) Å (N3–O1) (angle B1–N3–O1 115.4(1)°), which indicates that the boron heteroatom mainly inductively interacts with the radical moiety.

Crystallization of the obtained yellow solid from CH₂Cl₂/pentane gave the minor *B*-nitroxide radical compound **6a** as

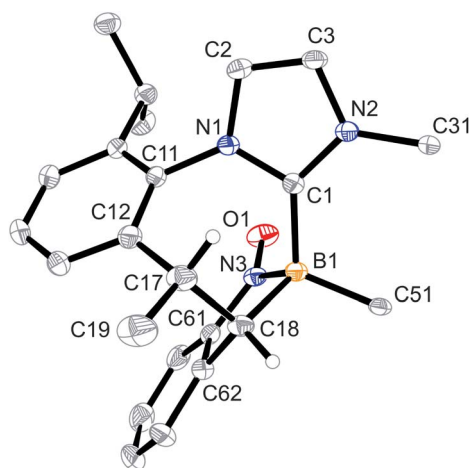


Fig. 3 A projection of the molecular structure of the boron-containing nitroxide radical **6a** [thermal ellipsoids are set at 30% probability; only the *ipso*-C₆F₅/Dipp carbon atoms C51/C31 are shown for clarity, and H atoms are omitted (except for C17H and C18H)]. Selected bond lengths (Å) and angles (°): B1–C1 1.633(3), B1–C18 1.649(3), B1–N3 1.563(3), C17–C18 1.570(3), N3–O1 1.289(2), N3–C61 1.386(3), B1–N3–O1 126.2(2), O1–N3–B1–C1 44.5(3), and $\Sigma N3^{BCO}$ 360.0.

orange crystals. The X-ray crystal structure analysis of compound **6a** shows the seven-membered core with the CHCH₃ moiety as the tip of the boat conformation (see Fig. 3). Adjacent to it is the newly formed annulated five-membered ring that contains the integrated NO radical functionality. This ring has an annulated phenylene moiety that originates from the nitrosobenzene reagent. We note that the B1–C1 bonds in radicals **5a** and **6a** are marginally longer than in compound **4a**.

Radicals **5a** and **6a** were characterized by C,H,N-elemental analysis and by CW-EPR spectroscopy. Fig. 4 (top) shows the EPR spectrum of compound **5a**. The EPR signal displays a *g*-factor of 2.0066 with a hyperfine-coupling with nitrogen [$A(^{14}\text{N})$ = 26.06 MHz], boron [$A(^{11}\text{B})$ = 12.50 MHz], and to the five hydrogen atoms of the phenyl substituent [$A(^1\text{H})$ = 6.31, 2.58, and 1.42 MHz]. The EPR spectrum of compound **6a** (Fig. 4, bottom) shows similar parameters (*g* = 2.00604 with hyperfine couplings: $A(^{14}\text{N})$ = 25.18 MHz, $A(^{11}\text{B})$ = 11.07 MHz, and $A(^1\text{H})$ = 9.65, 0.58, and 0.43 MHz). The hyperfine coupling constants $A(^{14}\text{N})$ of **5a** and **6a** are markedly smaller than found in the *N*-oxyl radicals TEMPO (43.5 MHz) or ^tBu₂NO (43.3 MHz).^{1,15} The $A(^{11}\text{B})$ values of the **5a/6a** pair are only slightly higher than what is reported for the P/B FLP-NO radical **IV** (9.1 MHz, see Scheme 1c).⁹ DFT calculations show that the spin density (probability that an unpaired electron is located at the nucleus) for radicals **5a** and **6a** resides on oxygen, nitrogen, boron, and the adjacent phenyl (**5a**) or phenylene (**6a**) groups (see ESI, Fig. S31†). Furthermore, the probability of an unpaired electron residing at ¹⁴N is higher than at ¹¹B in accordance with the observed EPR

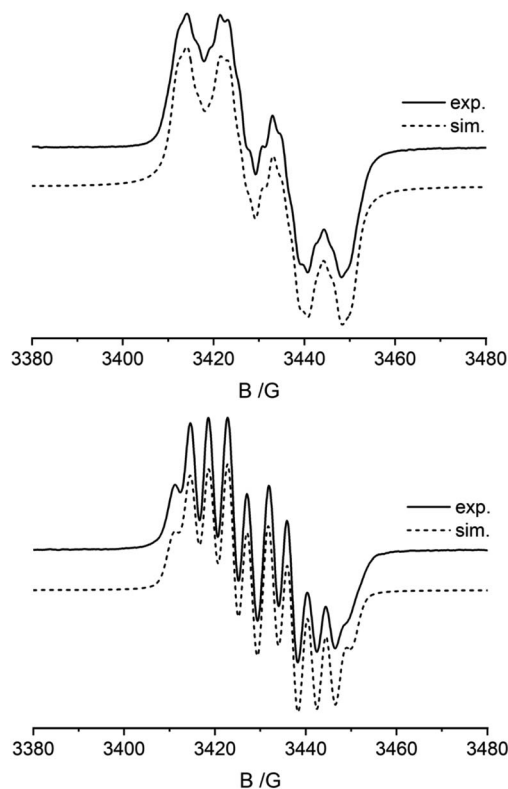


Fig. 4 Liquid state CW-EPR spectra (CH₂Cl₂, r.t.) and lineshape simulations of the *B*-nitroxide radicals **5a** (top) and **6a** (bottom). Tables S1 and S2† summarize the EPR lineshape simulation parameters.



parameters (see the ESI† for details; see Fig. S25† for the UV-vis spectra of compounds **5a** and **6a**).

The ratio of the radical products **5a** and **6a** vs. the [2 + 2] cycloaddition product **4a** is slightly solvent dependent. The highest radical yields were obtained from the reactions in benzene or toluene, whereas reactions in more polar solvents (acetonitrile or DMSO) gave smaller amounts of these nitroxide radicals (see the ESI† for details).

Boraalkene **3** was also reacted with the bulkier 2-nitrosotoluene. From this reaction, we obtained the [2 + 2] adduct **4b** in a yield of 80%. It was characterized spectroscopically and by C,H,N elemental analysis (see the ESI† for details). We could not isolate any of the respective nitroxide radicals **5b** or **6b** from this experiment. However, an EPR signal was recorded from the *in situ* experiment before workup. The spectrum in the ESI† indicates that radical **6b** was probably formed in this reaction, although as a very minor product.

The reaction of boraalkene **3** with the aliphatic 2-methyl-2-nitrosopropane reagent (D₆-benzene, 14 h, r.t.) took a similar course. Work-up furnished the [2 + 2] cycloaddition product **4c** in *ca.* 90% yield as a mixture of two persistent conformational isomers (**4c_{eq}** and **4c_{ax}**) in a *ca.* 3 : 1 molar ratio. A slow conformational isomerization was observed in solution, eventually resulting in the almost pure thermodynamic isomer **4c_{ax}** (see Scheme 4). This was characterised by X-ray diffraction (see Fig. 5). It shows a typical cycloheptatriene reminiscent boat shaped conformation of the central seven-membered ring with the methyl substituent at the C(sp³) tip oriented in an axial position. As in compound **4a**, the methyl substituent is *cis*-oriented to the annulated four-membered ring, only in the conformationally inverted situation. The *in situ* generated reaction solution showed an EPR signal of a minor as yet unidentified nitrogen containing radical component. The EPR spectrum is depicted in the ESI.†

For the mechanistic scheme leading to the formation of the persistent B–N-oxyl radicals **5a** and **6a**, we propose that this reaction occurs by a variant of the nitroso ene reaction, here the bora nitroso ene reaction (see Scheme 5). It had been discussed that two different essential types of intermediates may be involved in the nitroso ene reaction, namely an aziridine *N*-

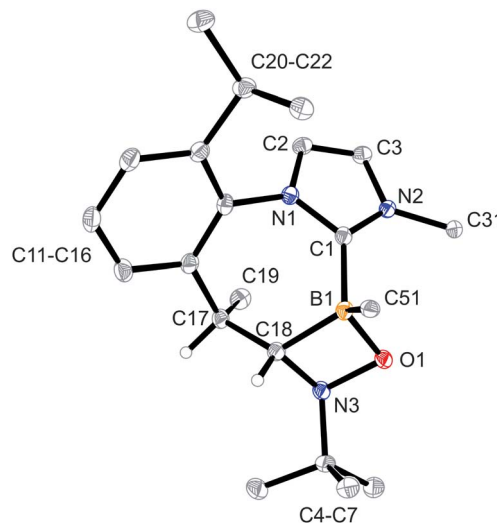
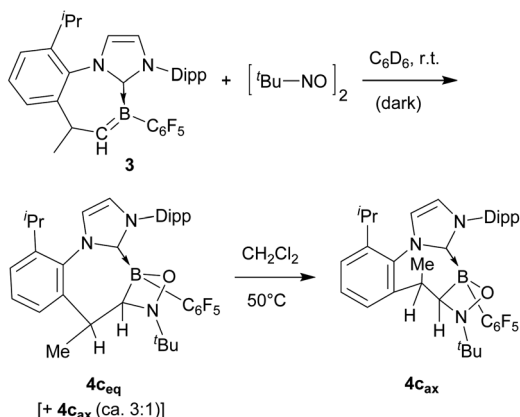


Fig. 5 A projection of the molecular structure of the **3** plus *t*Bu–NO [2 + 2] cycloaddition product **4c** [thermal ellipsoids are set at 30% probability; only the *ipso*-C₆F₅/Dipp carbon atoms C51/C31 are shown for clarity, and H atoms are omitted (except for C17H and C18H)]. Selected bond lengths (Å) and angles (°): B1–O1 1.495(3), B1–C1 1.635(3), B1–C18 1.636(3), N3–O1 1.497(3), N3–C18 1.496(3), and $\Sigma N3^{CCO}$ 319.6.

oxide^{10b} or a polarized diradical.^{10a} The diradical pathway would serve to explain the formation of both the isomeric nitroxide radicals **5a** and **6a** to potentially occur through the same intermediate. Compound **8** would be generated by nitroso arene coordination to boron through nitrogen. Subsequent internal H-abstraction would then directly give the bora nitroso ene product, the “boryl hydroxylamine” derivative **9** which is only one hydrogen atom transfer step from the obtained product **5a**. Apparently, the nitrosobenzene reagent serves as the H-acceptor to give **5a** and azoxybenzene (after H₂O elimination; see Fig. S61 in the ESI† for an *in situ* experiment on the generation of **5a** from **9**). In a competing reaction branch, the cyclic radical of conformer **10** of the diradical intermediate could attack the phenyl ring to generate intermediate **11**. Tautomerization would give the N–OH product **12** which would provide the observed product **6a** by its subsequent reaction with nitrosobenzene.

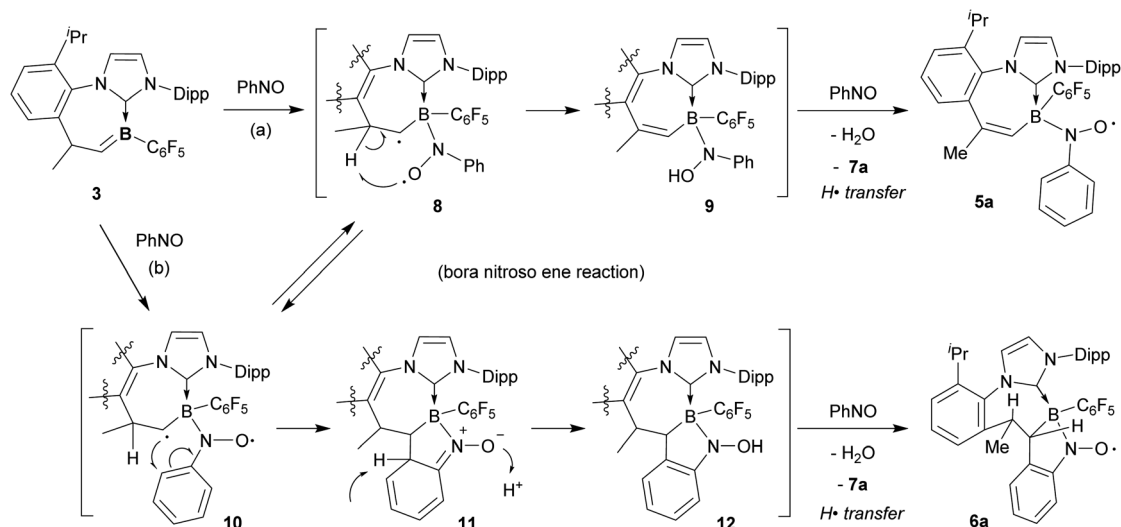
The newly formed products undergo some typical nitroxide radical reactions.¹ Compound **5a** readily abstracts a hydrogen atom from 1,4-cyclohexadiene to form the corresponding diamagnetic N–OH product **9** (see Scheme 6). It shows the ¹H NMR N–OH signal at δ 3.36 (in CD₂Cl₂ at 299 K) and a ¹¹B NMR resonance at δ –8.5. Compound **9** was characterized by X-ray diffraction. It shows very similar general structural parameters to its precursor **5a**, only the N3–O1 linkage in **9** is much longer at 1.467(2) Å (*cf.* 1.304(2) Å in **5a**). We also note that the C1–B1 linkage to the N-heterocyclic carbene ligand is slightly longer in radical **5a** (B1–C1 1.631(2) Å) than in the N–OH compound **9** (B1–C1 1.623(2) Å) (see the ESI† for the single crystal X-ray structure of compound **9**).

The boron substituent has an influence on the reactivity properties of the *B*-nitroxide radicals. Both the *B*-nitroxide

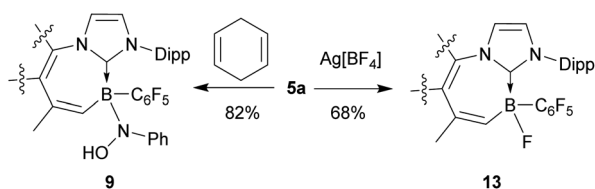


Scheme 4 Reaction of boraalkene **3** with 2-methyl-2-nitrosopropane.





Scheme 5 Possible pathways leading to the boryl nitroxide radicals **5a** and **6a**.



Scheme 6 Reactions of BNO radical **5a**.

radicals **5a** and **6a** are more easily oxidized than *e.g.* TEMPO. The cyclic voltammograms show redox features with $E_{1/2} = 0.53$ V for **5a** and 0.28 V for **6a** (rel. Ag/Ag^+), respectively [cf. TEMPO $E_{1/2} = 0.66$ V (rel. Ag/Ag^+)]; see the ESI† for details].¹⁶ We tried to oxidize radical **5a** to an oxoammonium cation by using $\text{Ag}[\text{BF}_4]$ as a chemical oxidant in CH_2Cl_2 (r.t., 30 min). After workup including flash chromatography (SiO_2), compound **13** was obtained as a white solid, and its structure was confirmed by X-ray single crystal analysis and by NMR spectroscopy (see the ESI† for details). This result indicates that the boryl NO radical indeed could be further oxidized, but the desired boryl oxoammonium cation was not stable under the reaction conditions; it underwent a substitution reaction to form the observed product **13**.

Radical **6a** was used in a Cu-catalyzed oxidation process of cinnamyl alcohol in a procedure similar to one described by Stahl *et al.*¹⁷ to give cinnamaldehyde. It turned out that the catalyst system derived from **6a** was slightly less active than the published system using the ubiquitous TEMPO radical (see the ESI† for details).

Conclusions

Boryl radical adducts of spin traps have been used to detect and characterize boron centred radicals.^{5–8} However, persistent boryl substituted nitroxide radicals that could be isolated and even characterized by X-ray crystal structure analysis are much less common.⁹ In this paper, we have

described the preparation of a pair of boron substituted nitroxide radicals that were isolated and characterized spectroscopically and by X-ray crystal structure analysis. The compounds **5a** and **6a** were obtained in a unique way by an analogue of the nitroso ene reaction, namely the bora nitroso ene reaction of a reactive cyclic boraalkene with nitrosobenzene. The EPR spectra have revealed that the spin density is affected by the presence of the boryl substituent at nitrogen. There are sizable $A(^{11}\text{B})$ coupling constants found for both the boryl nitroxide radicals **5a** and **6a**, and their $A(^{14}\text{N})$ coupling constants are markedly lower than *e.g.* for TEMPO. However, this effect is too small to show up in the structural data. The N–O· bond lengths of **5a** and **6a** (1.304(2) Å and 1.289(2) Å) fall within the same range as those of P/B FLPNO radical **IV** (1.297(2) Å) and the ubiquitous TEMPO radical (1.284(2) Å). First experiments indicate that this type of B–NO radical shows the typical nitroxide radical chemical behaviour, and we shall see if the incorporated *N*-boryl unit might lead to an extension of their reaction patterns.

Data availability

The ESI† contains experimental procedures, detailed analytical and structural data.

Author contributions

C. C. designed and performed the experiments, C. C. and G. K. analysed the experimental data, C. G. D. performed the X-ray crystal structure analysis, S. K. and M. R. H. performed the EPR measurements and data analysis, and G. E. supervised the project and wrote the paper with input from all authors.

Conflicts of interest

There are no conflicts to declare.



Acknowledgements

Financial support from the Deutsche Forschungsgemeinschaft is gratefully acknowledged. C. C. thanks the Alexander von Humboldt-Stiftung for a postdoctoral stipend.

Notes and references

- See for reviews: (a) L. Tebben and A. Studer, *Angew. Chem. Int. Ed.*, 2011, **50**, 5034; (b) J. E. Nutting, M. Rafiee and S. S. Stahl, *Chem. Rev.*, 2018, **118**, 4834; (c) H. A. Beeiapur, Q. Zhang, K. Hu, L. Zhu, J. Wang and Z. Ye, *ACS Catal.*, 2019, **9**, 2777. See also: (d) G. Moad and E. Rizzardo, Chapter 1: The History of Nitroxide-mediated Polymerization, in *Nitroxide Mediated Polymerization: From Fundamentals to Applications in Materials Science*, 2015, pp. 1–44.
- See for examples: (a) M. Shibuya, F. Pichierri, m. Tomizawa, S. Nagasawa and Y. Iwabuchi, *Tetrahedron Lett.*, 2012, **53**, 2070; (b) J. B. Gerken and S. S. Stahl, *ACS Cent. Sci.*, 2015, **1**, 234. See also: (c) R. Ciriminna and M. Pagliaro, *Org. Process Res. Dev.*, 2010, **14**, 245.
- See for examples: (a) K.-W. Huang and R. M. Waymouth, *J. Am. Chem. Soc.*, 2002, **124**, 8200; (b) J. J. Scepaniak, A. M. Wright, R. A. Lewis, G. Wu and T. W. Hayton, *J. Am. Chem. Soc.*, 2012, **134**, 19350; (c) Y.-L. Liu, G. Kehr, C. G. Daniliuc and G. Erker, *Organometallics*, 2017, **36**, 3407.
- S. L. Boyd and R. J. Boyd, *J. Phys. Chem.*, 1994, **98**, 1856.
- (a) M. P. Crozet and P. Tordo, *J. Am. Chem. Soc.*, 1980, **102**, 5696; see for comparison: (b) M. Lucarini, G. F. Pedulli and L. Valgimigli, *J. Org. Chem.*, 1996, **61**, 4309.
- H. Kaur, K. H. W. Leung, M. J. Perkins and J. C. S. Chem, *Comm*, 1981, 142.
- (a) J. A. Baban, V. P. J. Marti and B. P. Roberts, *Tetrahedron Lett.*, 1985, **26**, 1349; (b) V. P. J. Marti and B. P. Roberts, *J. Chem. Soc., Perkin Trans. 2*, 1986, 1613.
- (a) S.-H. Ueng, A. Solov'yev, X. Yuan, S. J. Geib, L. Fensterbank, E. Lacôte, M. Malacria, M. Newcomb, J. C. Walton and D. P. Curran, *J. Am. Chem. Soc.*, 2009, **131**, 11256; (b) X. Pan, E. Lacôte, J. Lalevée and D. P. Curran, *J. Am. Chem. Soc.*, 2012, **134**, 5669; (c) S. Telitel, A.-L. Vallet, S. Schweizer, B. Delpech, N. Blanchard, F. Morlet-Savary, B. Graff, D. P. Curran, M. Robert, E. Lacôte and J. Lalevée, *J. Am. Chem. Soc.*, 2013, **135**, 16938; (d) J. C. Walton, W. Dai and D. P. Curran, *J. Org. Chem.*, 2020, **85**, 4248; see for reviews: (e) T. Taniguchi, *Eur. J. Org. Chem.*, 2019, **2019**, 6308; (f) T. Yaniguchi, *Chem. Soc. Rev.*, 2021, **50**, 8995.
- (a) A. J. P. Cardenas, B. J. Culotta, T. H. Warren, S. Grimme, A. Stute, R. Fröhlich, G. Kehr and G. Erker, *Angew. Chem., Int. Ed.*, 2011, **50**, 7567; (b) M. Sajid, A. Stute, A. J. P. Cardenas, B. J. Culotta, J. A. M. Hepperle, T. H. Warren, B. Schirmer, S. Grimme, A. Studer, C. G. Daniliuc, R. Fröhlich, J. L. Petersen, G. Kehr and G. Erker, *J. Am. Chem. Soc.*, 2012, **134**, 10156. See also: (c) R. Liedtke, C. Eller, C. G. Daniliuc, K. Williams, T. H. Warren, M. Tesch, A. Studer, G. Kehr and G. Erker, *Organometallics*, 2016, **35**, 55.
- (a) A. G. Leach and K. N. Houk, *J. Am. Chem. Soc.*, 2002, **124**, 14820. See for a review: (b) W. Adam and O. Krebs, *Chem. Rev.*, 2003, **103**, 4131. For application of the nitroso ene reaction in organic synthesis, see for example: (c) J. Ouyang, R. Yan, X. Mi and R. Hong, *Angew. Chem., Int. Ed.*, 2015, **54**, 10940.
- C. Chen, J. Li, C. G. Daniliuc, C. Mück-Lichtenfeld, G. Kehr and G. Erker, *Angew. Chem., Int. Ed.*, 2020, **59**, 21460.
- (a) C. Chen, C. G. Daniliuc, G. Kehr and G. Erker, *Angew. Chem., Int. Ed.*, 2021, **60**, 19905; see also: (b) C. Chen, C. G. Daniliuc, G. Kehr and G. Erker, *J. Am. Chem. Soc.*, 2021, **143**, 21312; (c) K. Škoch, C. Chen, C. G. Daniliuc, G. Kehr and G. Erker, *Dalton Trans.*, 2022, **51**, 7695.
- D. A. Dieterich, I. C. Paul and D. Y. Curtin, *J. Chem. Soc. D*, 1970, 1710.
- J. R. Hwu, A. R. Das, C. W. Yang, J.-J. Huang and M.-H. Hsu, *Org. Lett.*, 2005, **7**, 3211.
- (a) Y. Maruyama, K. Nagamine, A. Nomura, S. Iwasa and S. Tokito, *Electrochemistry*, 2020, **88**, 34; (b) A. Dasgupta, E. Richards and R. L. Melen, *Angew. Chem., Int. Ed.*, 2021, **60**, 53.
- (a) T. Suga, Y.-J. Pu, K. Oyaizu and H. Nishide, *Bull. Chem. Soc. Jpn.*, 2004, **77**, 2203; (b) N. Frenzel, J. Hartley and G. Frisch, *Phys. Chem. Chem. Phys.*, 2017, **19**, 28841; (c) V. V. Pavlishchuk and A. W. Addison, *Inorg. Chim. Acta*, 2000, **298**, 97.
- J. M. Hoover and S. S. Stahl, *J. Am. Chem. Soc.*, 2011, **133**, 16901.

